Rapid Communications

Microscopic reweighting for nonequilibrium steady-state dynamics

Marius Bause,* Timon Wittenstein, Kurt Kremer, and Tristan Bereau
Max Planck Institute for Polymer Research, 55128 Mainz, Germany

(Received 10 July 2019; published 19 December 2019)

Computer simulations generate trajectories at a single, well-defined thermodynamic state point. Statistical reweighting offers the means to reweight static and dynamical properties to different equilibrium state points by means of analytic relations. We extend these ideas to nonequilibrium steady states by relying on a maximum path entropy formalism subject to physical constraints. Stochastic thermodynamics analytically relates the forward and backward probabilities of any pathway through the external nonconservative force, enabling reweighting both in and out of equilibrium. We avoid the combinatorial explosion of microtrajectories by systematically constructing pathways through Markovian transitions. We further identify a quantity that is invariant to dynamical reweighting, analogous to the density of states in equilibrium reweighting.

DOI: 10.1103/PhysRevE.100.060103

Many chemical and biological processes are influenced by external driving forces and operate away from equilibrium—examples include colloidal particles, biopolymers, enzymes, and molecular motors [1]. Despite our current lack of a universal theory for statistical mechanics off equilibrium [2], computer simulations can complement experiments by providing microscopic insight into these complex processes. Unfortunately, current computational power often prevents molecular simulations from reaching the experimentally relevant timescales or, alternatively, obliges them to operate at artificially large driving forces [3]. The latter motivates a formalism to reweight dynamics across off-equilibrium conditions.

When dealing with systems in equilibrium, Ferrenberg and Swendsen introduced a statistical-reweighting procedure to infer information about a system when sampled at another state point [4,5]. It requires microscopic information at fixed thermodynamic conditions, e.g., temperature, collected by computer simulations or experiments. A probability associated with each microstate is reweighted according to physical relationships linking the initial and final thermodynamic conditions. Reweighting can be conducted arbitrarily far from the initial state, provided it is sufficiently sampled.

Equilibrium reweighting has led to a number of developments in the field, from estimating accurate free energies [6] to building more robust Markov state models [7,8]. In this Rapid Communication, we generalize reweighting to dynamical processes by replacing microstates with microtrajectories. The proposed methodology, valid for nonequilibrium steady-state (NESS) systems, employs a maximum path entropy formalism while generalizing the standard detailed balance relation.

Jaynes' maximum entropy approach offers a general variational principle to understand macroscopic phenomena from microscopic knowledge of a statistical system [9]. This information-theoretic method regards entropy as the measure of uncertainty of the system. Consider a coordinate x of a system with unknown probability distribution, $p(x)$. We further define another distribution, $q(x)$, used as a prior on $p(x)$. The most likely representation of $p(x)$ can be found by minimizing the cross-entropy functional

$$\mathcal{C}[p(x)] = -\int dx\; p(x) \ln\left[\frac{p(x)}{q(x)}\right]. \tag{1}$$

This quantity was shown to fulfill the axioms for an uncertainty measure [10]. Setting a uniform prior (i.e., $q(x) =$ const.) reduces to the well-known Shannon entropy and minimizing the cross entropy in this case is equivalent to maximizing the Shannon entropy.

According to Jaynes, a system would maximize the number of microscopic realizations compatible with a certain macroscopic state, linking the two scales via constraints. For instance, working in the canonical ensemble will lead to a constraint on the average energy $\langle E \rangle$

$$\mathcal{C}_{\text{equ}} = -\int dx\; p(x) \ln\left[\frac{p(x)}{q(x)}\right] - \zeta\left(\int dx\; p(x) - 1\right) - \beta\left(\int dx\; p(x)E(x) - \langle E \rangle\right), \tag{2}$$

where ζ and β are Lagrangian multipliers, controlling the normalization of probabilities and the fixed average energy. Minimization of $\mathcal{C}_{\text{equ}}$ with respect to $p(x)$ yields

$$p(x) = \frac{q(x)}{\tilde{Z}(\beta)} \exp\left[-\beta E(x)\right], \tag{3}$$

where the partition function $\tilde{Z}(\beta) = \int dx\, q(x) \exp\left[-\beta E(x)\right]$ becomes a normalization constant and the Lagrange multiplier β is identified with the inverse temperature, $\beta^{-1} = k_{\text{B}}T$. This approach naturally lends itself to reweighting: Given a reference distribution $q(x)$ sampled at inverse temperature β', microscopic information at a third inverse temperature $\beta'' = \beta + \beta'$ is inferred through the calculation of $p(x)$. This reweighting becomes exact under full knowledge of the density of states function $\Omega(x) = q(x) \exp\left[\beta' E(x)\right]$.

*bause@mpip-mainz.mpg.de

The maximum entropy formalism has been generalized to the study of dynamical systems by working with microtrajectories—an approach called maximum caliber [11]. It was shown to recover known off-equilibrium relations [12] and predict dynamical pathways in NESSs correctly when supplied with appropriate constraints [13]. Conceptually, the approach follows the same scheme as the previous derivation of equilibrium reweighting: The most likely microtrajectories maximize the path entropy function subject to physical constraints.

The following discusses a rich and relevant subset of nonequilibrium processes: nonequilibrium steady states. NESS correspond to the long-time limit under constant driving by an external reservoir [14]. As such, time symmetry is broken, but the fluxes within the system are time independent and so are the distributions of microtrajectories.

Compared to equilibrium reweighting that focuses on the sampling of microstates, dynamical reweighting of NESS considers microtrajectories—collections of microstates—which become computationally intractable for all but the smallest of systems. To complicate things further, the length of time of a microtrajectory is *a priori* unknown. To resolve these issues, we map all trajectories to a first-order Markov process. This coarse graining of microtrajectories leaves us with the easier task of sampling transition probabilities and subsequently *constructing* microtrajectories out of the combination of individual microtransitions. Such an approach facilitates the sampling of microtrajectories.

Markov state models (MSM) discretize configurational space into so-called microstates (i.e., collection of microscopic states) as well as time in terms of steps of constant length τ (i.e., the lag time), thereby mapping trajectories to a discrete-time Markov chain [15]. All observed transitions are collected to infer a transition probability matrix $p_{ij}(\tau)$, where i and j label microstates. An appropriate space and time discretization helps fulfill the Markovian assumption [16]. Markov state models have proven powerful tools for reaching timescales that are unattainable by brute-force computer simulations [17].

Utilizing the Markovian assumption, the microtrajectories of the abovementioned cross-entropy functional [Eq. (1)] reduce to

$$\mathcal{C} = -\sum_{i,j} \pi_i p_{ij} \ln \frac{p_{ij}}{q_{ij}}, \tag{4}$$

where π corresponds to the stationary distribution [18]. In the absence of constraints, the minimum of the cross entropy is its prior q_{ij}.

Previous work has shown how to constrain the system according to microscopic and/or macroscopic constraints in equilibrium: (i) the matching of simulation and experimental data at equilibrium by enforcing detailed balance [19,20]; (ii) inferring kinetic rates given variations in equilibrium populations [21]; or (iii) by using the stationary distribution and macroscopic constraints [22]. Such macroscopic constraints are typically process dependent and are not always known. Turning to NESS can lead to more severe consequences: Macroscopic constraints displaying symmetry often impose space inversion and time reversal, resulting in nondissipative ensembles [23]. Instead, the modeling of dissipative NESS systems requires constraints that are antisymmetric or without symmetry [13]. Still, macroscopic constraints alone are unable to describe the dynamics correctly [24]: A system can be driven globally or only at the boundaries and can globally dissipate the same amount of heat while showing different dynamics. In this Rapid Communication, we propose to constrain the dynamics of a NESS to antisymmetric and *microscopic* balance constraints. We account for these effects by drawing antisymmetric *microscopic* balance constraints from microscopic reversibility [25,26]

$$\frac{\mathcal{P}[\Gamma(+t)|f(+t)]}{\mathcal{P}[\bar{\Gamma}(-t)|\bar{f}(-t)]} = \exp\left(-\beta Q|\Gamma(+t)|f(+t)]\right), \tag{5}$$

where $\mathcal{P}[\Gamma(+t)|f(+t)]$ denotes the probability of observing the time-forward trajectory $x(+t)$ under the external driving force $f(+t)$, $\mathcal{P}[\bar{\Gamma}(-t)|\bar{f}(-t)]$ points at the time-reversed trajectory, while $Q[\Gamma(+t)|f(+t)]$ refers to the amount of heat exchanged between the system and the reservoir along a given trajectory and acting forces. Critically, this links the probability of a forward trajectory with its time-reversed counterpart. In the case of equilibrium dynamics, the relation becomes path independent and simplifies to detailed balance [27]. For a more general expression, we integrate Eq. (5) over the complete set of initial states i, target states j, as well as the set of all trajectories connecting them, to obtain the coarser expression [24],

$$\langle \Delta S_{ij} \rangle = \ln \frac{p_{ij}}{p_{ji}}, \tag{6}$$

where ΔS_{ij} is called local entropy production, describing the amount of work an external reservoir has to perform on the system to transition between two states. This quantity naturally generalizes detailed balance [28] and will be used as a microscopic constraint on the caliber.

Furthermore, we consider a set of global constraints: The conservation of probability flow through so-called global balance, $\sum_i \pi_j p_{ji} = \sum_i \pi_i p_{ij}$, allowing for global fluxes in the system. Normalization considerations imply $\sum_j p_{ij} = 1$ and $\sum_i \pi_i = 1$. Since all transition probabilities in NESSs are time independent, the existence of a steady-state distribution π is guaranteed [29,30].

Having defined all constraints, the caliber functional becomes

$$\mathcal{C}_{\mathrm{dyn}} = \underbrace{-\sum_{i,j} \pi_i p_{ij} \ln \frac{p_{ij}}{q_{ij}}}_{\text{Caliber}} + \underbrace{\sum_i \mu_i \left(\sum_j p_{ij} - 1 \right) + \zeta \sum_i (\pi_i - 1)}_{\text{Normalization}} + \underbrace{\sum_j \nu_j \left(\sum_i \pi_i p_{ij} - \pi_j \right)}_{\text{Global Balance}} + \underbrace{\sum_{ij}^{i<j} \pi_i \alpha_{ij} \left(\ln \left(\frac{p_{ij}}{p_{ji}} \right) - \Delta S_{ij} \right)}_{\text{Local Balance}}, \tag{7}$$

where μ_i, ζ, ν_j, and α_{ij} are Lagrange multipliers. Equation (7) modifies the equilibrium-reweighting caliber [Eq. (2)] in several ways: (i) The entropy expression is discretized and replaced by the path entropy; (ii) transition probabilities are normalized; (iii) a global-balance condition ensures a steady state; and (iv) local entropy production is introduced as a NESS extension to detailed balance. The solution is obtained by minimizing with respect to the set of transition probabilities and the stationary distribution. Assuming that ΔS_{ij} is small [24], we obtain

$$p_{ij} = q_{ij} \exp\left(\frac{c_i + c_j}{2} + \frac{\Delta S_{ij} - \Delta S_{ij}^q}{2} + \zeta\right), \tag{8}$$

which only depends on $\Delta S_{ij}^q = \ln(q_{ij}/q_{ji})$ from the reference simulation, ΔS_{ij}, and the unknown constants c_i [24]. We note that ΔS_{ij} corresponds to the local entropy production in the target state. Analogous to histogram reweighting, the unknown coefficients c_i can be found via nonlinear relationships [31]

$$1 = \sum_j p_{ij} = \sum_j \sqrt{q_{ij} q_{ji}} \exp\left(\frac{c_i + c_j + 2\zeta}{2} + \frac{\Delta S_{ij}}{2}\right). \tag{9}$$

The set of equations is convex [24] and is solved by self-iteration from a randomly selected starting point until convergence.

An alternative formalism by means of the Girsanov theorem was introduced, which relies on single-trajectory probability reweighting and the Boltzmann distribution to estimate the change between equilibrium state points [32]. In another work, equilibrium transition rates are reweighted by a maximum caliber formalism enforcing the Boltzmann distribution [21]. In contrast, the present method reweights MSMs in NESS without prior knowledge of the steady-state distribution, but rather through the entropy production.

Application. The reweighting procedure is tested on a single particle driven by a nonconservative force f along a periodic one-dimensional potential $U(x)$ (see Fig. 1). The nonconservative force may emerge from magnetic fields, mechanical flows, or mechanical dragging. An analogous setup was experimentally studied, using silica spheres on a tilted surface [33]. The overdamped equation of motion for the particle is given by

$$0 = -\frac{\partial U(x)}{\partial x} - \gamma \dot{x} + \sqrt{2\gamma k_B T} R(t) + f, \tag{10}$$

where T is the temperature of a canonical reservoir coupled to the system by friction constant γ. $R(t)$ is a δ-correlated Gaussian process with mean 0. Both the temperature and the potential energy are fixed, while the reweighting is performed over different ranges of nonconservative forces. We report results in reduced units, where the box size is set to $\mathcal{L}$, the mass of the particle is set to $\mathcal{M}$, and energy is measured in ϵ. The temperature is chosen to be $T = 1\,\epsilon/k_B$, and the energy barriers shown in Fig. 1 are $2\,k_B T - 4\,k_B T$. Following our Markovian approximation, the model is separated in 60 microstates of equal size and a lagtime $\tau = 2 \times 10^{-3}\mathcal{T}$, where $\mathcal{T} = \mathcal{L}\sqrt{\mathcal{M}/\epsilon}$ is the unit of time. The integration time step

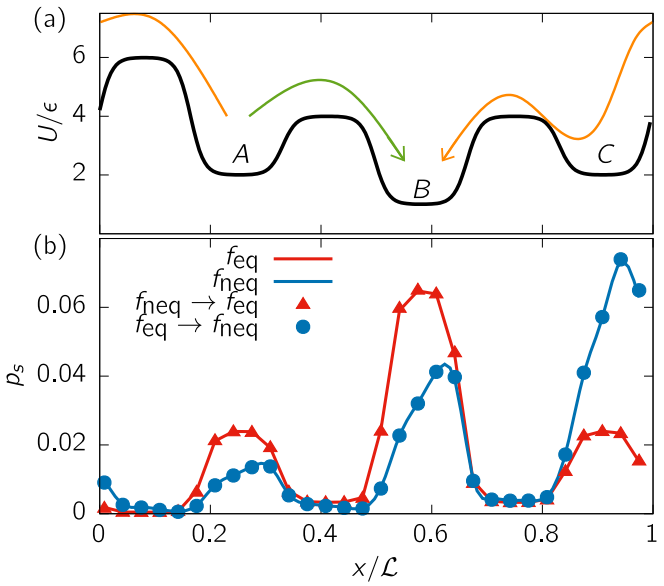

FIG. 1. (a) Periodic potential energy surface experienced by the particle. The two arrows show possible paths from metastable state A to B. (b) Stationary distributions for the equilibrium reference system, $f_{eq} = 0$ (red, symmetric distribution), and under the influence of a nonconservative driving force, $f_{neq} = 9\epsilon/\mathcal{L}$ (blue, asymmetric distribution). The points show the probability distributions obtained by sampling in one of the two states and reweighting into the other, $f_{neq} \to f_{eq}$ and $f_{eq} \to f_{neq}$.

was set to $\delta t = 10^{-5}\,\mathcal{T}$. The nonconservative force is varied between 0 and $9\epsilon/\mathcal{L}$.

For the given model, we want to derive an analytic expression for the local entropy productions ΔS_{ij}, required by the reweighting procedure [Eq. (8)]. Given an underlying force field $\mathbf{F} = -\nabla U(x) + \mathbf{f}$, the local entropy production of a single continuous trajectory $\mathbf{\Gamma}(t)$ is given by

$$\Delta S[\Gamma(t)] = \int dt \frac{\mathbf{F} \cdot \dot{\mathbf{\Gamma}}}{T}, \tag{11}$$

where the quantity is integrated over time, $\dot{\mathbf{\Gamma}}$ is the velocity, and T is the temperature [34]. Assuming a constant nonconservative force $\mathbf{f}$ and making use of a numerically discretized trajectory, $\mathbf{\Gamma}(t) \approx \{\mathbf{x}_k\}$, we approximate ΔS between starting and target points x_i and x_j, respectively,

$$\Delta S_{ij}(\{\mathbf{x}_k\}) \approx \frac{U(x_i) - U(x_j) + \sum_k (\mathbf{x}_{k+1} - \mathbf{x}_k) \cdot \mathbf{f}}{k_B T}. \tag{12}$$

Because the entropy production of forward and backward steps directly cancel, the quantity is unaffected by path variations in one dimension. Still, the periodic boundary conditions permit two different results between i and j, as indicated in Fig. 1, the shorter and longer paths (green and orange, respectively), such that Eq. (12) has two solutions. By choosing the lag time of the MSM to be reasonably short, we effectively scale down the longer paths to a negligible weight. As such, our expression for the local entropy production becomes

$$\Delta S_{ij} \approx \frac{U(x_i) - U(x_j) + (x_j - x_i) f}{k_B T}. \tag{13}$$

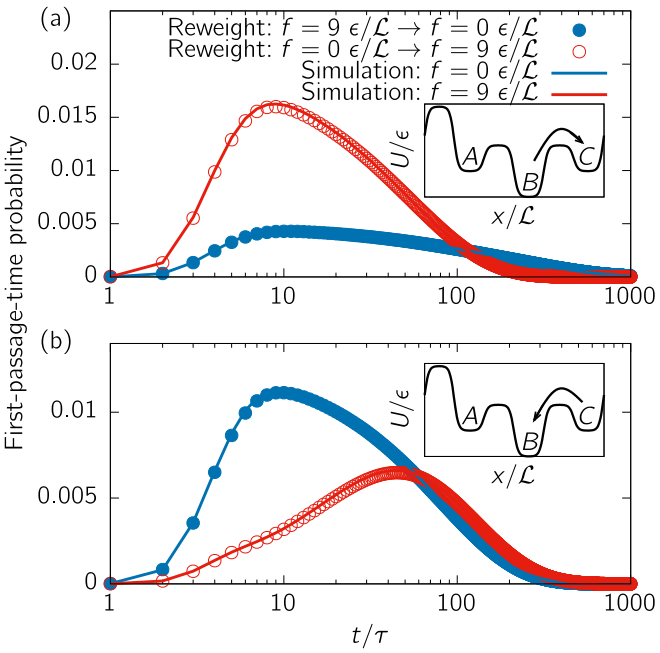

FIG. 2. First passage time probabilities between metastable states B and C, expressed as a function of time (in units of the lag time τ). The lines show the simulation data at $f = 0$ and $f = 9\,\epsilon/\mathcal{L}$. The points show the results under reweighting from each other for processes (a) $B \to C$ and (b) $C \to B$.

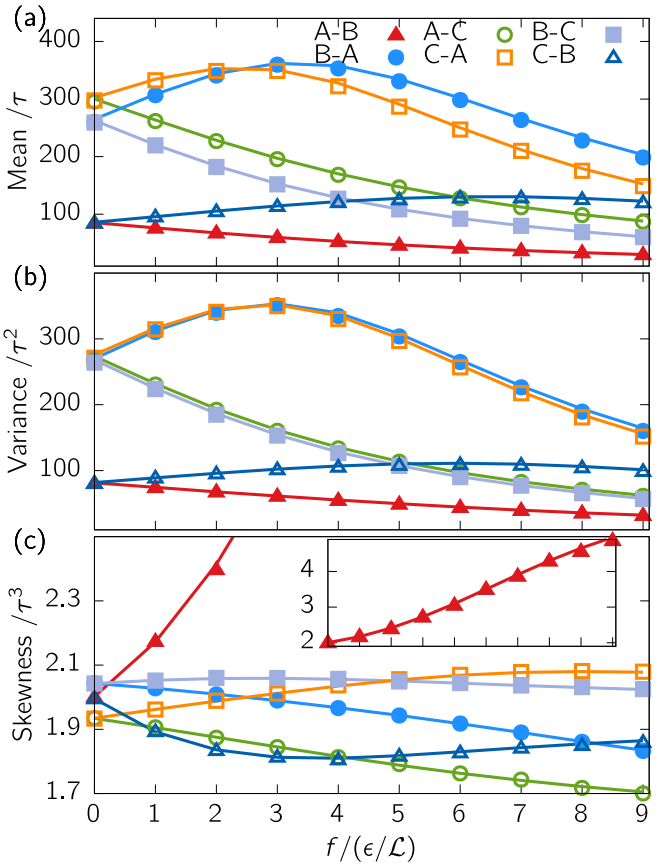

FIG. 3. Moments of the first-passage-time distribution between three metastable states under external driving: (a) mean, (b) variance, and (c) skewness. The metastable states are defined in Fig. 1. The points correspond to reference simulations at various states, while the lines show the quantity under continuous reweighting, always choosing the equilibrium system ($f = 0$) as reference.

The expression depends on temperature—a quantity that may change in off-equilibrium systems due to driving of an off-equilibrium reservoir [35]. Here we find excellent agreement between the expression in Eq. (13) using the equilibrium-reservoir temperature and Eq. (6) when directly sampled from an MSM: a weighted average error of 1%, which does not affect the quality of the reweighting upon insertion in Eq. (8) [24]. We conclude that the derived equation holds, effectively implying weak coupling between the driving force and temperature. Such a coupling might become relevant for more complex systems.

To assess our reweighting procedure, we monitor both static and kinetic properties: (i) the stationary distribution of the particle position and (ii) the first-passage-time distributions between metastable states. The metastable states are labeled A, B, and C (Fig. 1).

Figure 1 shows the stationary distributions of the particle position both in equilibrium and under the influence of a driving force. We reweight the simulation data from equilibrium to the NESS and vice versa, demonstrating that the correct static distributions are recovered when reweighting both in and out of equilibrium—a result that holds for any pair of state points as described further below.

Turning to dynamical properties, Fig. 2 reports the first-passage-time distributions between two metastable states in equilibrium and under a strong global driving force ($f = 9\epsilon/\mathcal{L}$). The change in the broadness of the distributions [Fig. 2(a)] and the shift in the peak position [Fig. 2(b)] suggest that the set of dominant trajectories change significantly under driving. This example shows that the external driving force changes both the timescale and corresponding processes of a transition. Here again, the reweighting procedure recovers the first-passage-time distributions in either directions: from equilibrium to NESS and vice versa.

This analysis is extended to other state points by comparing the mean, variance, and skewness of the first-passage-time distributions in Fig. 3. The equilibrium system is chosen as a reference and is continuously reweighted to off-equilibrium driven systems, even though any other reference state point could be selected. Additionally, we validate our reweighting procedure using two other systems: (i) an equilibrium system obtained by varying the potential [24] and (ii) an off-equilibrium system motivated by a four-state laser model using a locally constrained nonconservative force, as a way to illustrate population inversion [24,36].

The present reference potential energy surface in Fig. 1 [24] is such that several pairs of processes show the same dynamics at equilibrium: the transition $A \to B$ and $C \to B$, but also $B \to A$ and $B \to C$ as well as $A \to C$ and $C \to A$.

Upon driving the system off equilibrium, these symmetries break—a phenomenon captured by the reweighting procedure. Increasing f strongly affects the mean-first-passage times (Fig. 3), thereby altering the nature of the slowest processes. We first analyze the metastable transitions situated

along the direction of f. While the processes $A \to B$ and $B \to C$ speed up with increasing driving, $C \to A$ shows a nonmonotonic behavior: It first slows down up to a driving force $f \approx 4\,\epsilon/\mathcal{L}$ before speeding up. The variance reveals that a broader selection of trajectories becomes dominant before the threshold. Turning to metastable transitions that oppose to the driving force, only the process $C \to B$ slows down with driving, while $A \to C$ constantly speeds up, despite unfavorable driving. Process $B \to A$ shows nonmonotonic behavior, similar to $C \to A$. This counterintuitive behavior can be explained by the growing number of long transitions from B to A via C.

Reweighting implies the existence of an invariant quantity, irrespective of the state point or driving force. Here we can isolate the following invariant $I_{ij} = \sqrt{q_{ij}q_{ji}}\exp\left(\frac{c_i+c_j}{4}+\zeta\right)$ [24]. The invariant is symmetric under time-space inversion and thus preserves nondissipative information about the system [36]. We can thereby rewrite the abovementioned solution of the caliber [Eq. (8)] as

$$p_{ij} = \frac{I_{ij}}{Z_{ij}}\exp\left(\frac{\Delta S_{ij}}{2}\right), \tag{14}$$

using the normalization $Z_{ij} = \exp\left(\frac{-c_i-c_j}{4}\right)$. Note that Z_{ij} depends on both I_{ij} and ΔS_{ij} via the relation $1 = \sum_j \frac{I_{ij}}{Z_{ij}}\exp\left(\frac{\Delta S_{ij}}{2}\right)$ and accounts for the interconnection of the states. We draw similarities with equilibrium reweighting in Eq. (3): (i) The probability is proportional to the product of an invariant and an exponential function (the density of states and the Boltzmann factor in equilibrium); (ii) the partition function depends on the control variable (T or ΔS_{ij}); and (iii) the reweighting only depends on *relative* quantities, only requiring knowledge of temperature difference or changes in the local entropy production. Both procedures show striking similarities in their derivation, functional form, and properties.

The present reweighting method is a generalization of existing likelihood and maximum caliber methods that have been applied to systems in and out of equilibrium with varying microscopic and macroscopic constraints. The microscopic expression for the local entropy production acts as a local constraint that generalizes detailed balance for NESS. We show that this choice governs static and dynamic properties of a NESS and enables us to reproduce these properties over a wide range of driving. The analytic expression for the relative entropy production allows us to continuously tune the external driving force and quantitatively reweight the stationary distribution and kinetic properties. Critically, we reduce the combinatorial explosion of pathways by connecting our approach to Markov state models, thereby *constructing* microtrajectories from individual microtransitions.

The maximum caliber formalism in combination with local entropy productions offer an analytic relation between NESSs. Dynamical data of a system can be gathered in a driving-invariant quantity and detailed kinetic information at any thermodynamic state point can be recovered. This idea allows us to populate rare transition paths [37]: A driving force may push the system to discover new paths and the reweighting procedure recovers detailed dynamical information of the sampled path at any another thermodynamic state point. In case equilibrium dynamics are of interest, the entropy productions only depend on the free energy. Low-weight trajectories can thus be calculated with high accuracy and no further information. By tuning the relative local entropy productions of the system, the reweighting allows us to study dynamical properties and pathways in NESS without further simulation.

We thank Joseph F. Rudzinski, Dominik Spiller, and Johannes Zierenberg for insightful discussions. This work was supported in part by the Emmy Noether program of the Deutsche Forschungsgemeinschaft (DFG) to T.B., the Graduate School of Excellence Materials Science in Mainz (MAINZ) to M.B., and in part by the European Research Council under the European Union's Seventh Framework Programme (FP7/2007-2013)/ERC Grant Agreement No. 340906-MOLPROCOMP to K.K.

[1] U. Seifert, Eur. Phys. J. B **64**, 423 (2008).
[2] J. P. Dougherty, Philos. Trans. R. Soc. London A **346**, 259 (1994).
[3] J. R. Perilla, B. C. Goh, C. K. Cassidy, B. Liu, R. C. Bernardi, T. Rudack, H. Yu, Z. Wu, and K. Schulten, Curr. Opin. Struct. Biol. **31**, 64 (2015).
[4] A. M. Ferrenberg and R. H. Swendsen, Phys. Rev. Lett. **61**, 2635 (1988).
[5] A. M. Ferrenberg and R. H. Swendsen, Comput. Phys. **3**, 101 (1989).
[6] S. Kumar, J. M. Rosenberg, D. Bouzida, R. H. Swendsen, and P. A. Kollman, J. Comput. Chem. **13**, 1011 (1992).
[7] J. D. Chodera, W. C. Swope, F. Noé, J.-H. Prinz, M. R. Shirts, and V. S. Pande, J. Chem. Phys. **134**, 244107 (2011).
[8] H. Wu, A. S. Mey, E. Rosta, and F. Noé, J. Chem. Phys. **141**, 214106 (2014).
[9] E. T. Jaynes, Phys. Rev. **106**, 620 (1957).
[10] J. Shore and R. Johnson, IEEE Trans. Inf. Theory **26**, 26 (1980).
[11] E. T. Jaynes, Annu. Rev. Phys. Chem. **31**, 579 (1980).
[12] P. D. Dixit, J. Wagoner, C. Weistuch, S. Pressé, K. Ghosh, and K. A. Dill, J. Chem. Phys. **148**, 010901 (2018).
[13] L. Agozzino and K. Dill, Phys. Rev. E **100**, 010105(R) (2019).
[14] R. Zia and B. Schmittmann, J. Stat. Mech.: Theory Exp. (2007) P07012.
[15] G. R. Bowman, V. S. Pande, and F. Noé (eds.), *An Introduction to Markov State Models and Their Application to Long Timescale Molecular Simulation*, Advances in Experimental Medicine and Biology, Vol. 797 (Springer, Heidelberg, Germany, 2014).
[16] J.-H. Prinz, H. Wu, M. Sarich, B. Keller, M. Senne, M. Held, J. D. Chodera, C. Schütte, and F. Noé, J. Chem. Phys. **134**, 174105 (2011).
[17] N. Plattner, S. Doerr, G. De Fabritiis, and F. Noé, Nat. Chem. **9**, 1005 (2017).
[18] J. Lee and S. Pressé, J. Chem. Phys. **137**, 074103 (2012).
[19] J. F. Rudzinski, K. Kremer, and T. Bereau, J. Chem. Phys. **144**, 051102 (2016).

[20] P. D. Dixit and K. A. Dill, J. Chem. Theory Comput. **14**, 1111 (2018).
[21] H. Wan, G. Zhou, and V. A. Voelz, J. Chem. Theory Comput. **12**, 5768 (2016).
[22] P. D. Dixit, A. Jain, G. Stock, and K. A. Dill, J. Chem. Theory Comput. **11**, 5464 (2015).
[23] R. L. Jack and R. Evans, J. Stat. Mech.: Theory Exp. (2016) 093305.
[24] See Supplemental Material at http://link.aps.org/supplemental/10.1103/PhysRevE.100.060103 for derivations, additional results, and test of macroscopic constraints.
[25] G. E. Crooks, J. Stat. Mech.: Theory Exp. (2011) P07008.
[26] G. E. Crooks, J. Stat. Phys. **90**, 1481 (1998).
[27] X.-J. Zhang, H. Qian, and M. Qian, Phys. Rep. **510**, 1 (2012).
[28] C. Maes, K. Netočný, and B. Wynants, Markov Proc. Rel. Fields. **14**, 445 (2008).
[29] D. J. Evans, D. J. Searles, and S. R. Williams, J. Chem. Phys. **132**, 024501 (2010).
[30] D. J. Evans, S. R. Williams, D. J. Searles, and L. Rondoni, J. Stat. Phys. **164**, 842 (2016).
[31] T. Bereau and R. H. Swendsen, J. Comput. Phys. **228**, 6119 (2009).
[32] L. Donati, C. Hartmann, and B. G. Keller, J. Chem. Phys. **146**, 244112 (2017).
[33] X.-g. Ma, Y. Su, P.-Y. Lai, and P. Tong, Phys. Rev. E **96**, 012601 (2017).
[34] U. Seifert, Phys. Rev. Lett. **95**, 040602 (2005).
[35] C. Maes, J. Stat. Phys. **154**, 705 (2014).
[36] C. Maes, *Nondissipative Effects in Nonequilibrium Systems* (Springer, Berlin, 2018).
[37] P. G. Bolhuis, D. Chandler, C. Dellago, and P. L. Geissler, Annu. Rev. Phys. Chem. **53**, 291 (2002).